

JOURNAL OF MECHANICS OF CONTINUA AND **MATHEMATICAL SCIENCES**

www.journalimcms.org



ISSN (Online): 2454 -7190 Vol.-20, No.-11, November (2025) pp 124-139 ISSN (Print) 0973-8975

DESIGN A NON-COHERENT MULTI-CARRIER CHAOTIC SYSTEM BASED ON GENERALIZED CARRIER AND PERMUTATION INDEXES MODULATION MECHANISM

Ban M. Alameri¹, Aya Jamal Kamal² and Lubna Abbas Ali³

^{1,2} Department of Electrical Engineering, Mustansiriyah University, College of Engineering, Baghdad, Iraq.

³Department of Computer Engineering, Mustansiriyah University, College of Engineering, Baghdad, Iraq.

Email: ¹ban.alameri@uomustansiriyah.edu.iq, ²a.jamalkamal@yahoo.com, ³lubna altememi@uomustansiriyah.edu.iq

Correspondence: Ban M. Alameri

https://doi.org/10.26782/jmcms.2025.11.00008

(Received: August 14, 2025; Revised: October 22, 2025; November 07, 2025)

Abstract

This study introduces a novel system called Generalized Joint Permutation-Carrier Index Modulation Based MC-DCSK (GJPC-IM-MCDCSK) aimed at enhancing energy efficiency, spectral efficacy, and data transmission rates of GCI-DCSK technology by generating and utilizing permuted forms of the reference chaotic series with quasi-orthogonal properties to distribute the modulated bits across each operational carrier. Furthermore, rather than employing correlation detection, the receiving end of the proposed system utilizes greedy detection to streamline the process. Evaluating the data rate, spectral efficiency, and complexity of the proposed GJPC-IM-MCDCSK system against GCI-DCSK, CI-DCSK1, and MC-DCSK technologies illustrates the superior performance of the recommended design. To illustrate the proposed design's superiority, the simulated Bit Error Rate (BER) performance is evaluated for the GJPC-IM-MCDCSK scheme and compared with the GCI-DCSK, CI-DCSK1, and MC-DCSK systems under AWGN and multipath Rayleigh fading channels.

Keywords: Active carrier, permutation, Index, greedy detection, correlation detection

I. Introduction

Aperiodic chaotic patterns, which may be easily created by minimal power consumption and inexpensive devices, bring significant properties and qualities that motivate the utilization of chaos in the framework of radio communication and chaotic modulation schemes [XXXI]. Chaotic waves are useful for many spreadspectrum modulating devices due to their broadband spectral features and significant cross and autocorrelation benefits. On top of that, it can withstand degradation caused by multipath fading conditions. Its noise-like signal and aperiodic nature also make it

a potential contender for usage in military applications, since they allow for safer communication [III]. The need for coherent or non-coherent communications networks based on a chaotic modulator is dictated by the requirements for receiver and transmitter synchronization and estimation for channel state. In order to be coherent, an arrangement such as chaotic shift keying (CSK) has to be able to synchronize and estimate channel information. Dealing with an obstructed channel might be challenging. However, because the receiving end does not require synchronization or estimation of the channel's details procedure in order to retrieve the message, non-coherent chaotic modulation schemes, including DCSK, which symbolizes differential chaos shift keying, have attracted a lot of attention [XXI]. There are actually two identical time intervals in the DCSK signal period [XVIII, XXXII]. The reference chaotic series is communicated in the primary time position, and either an identical or an opposite copy of the reference wave is delivered in the subsequent time interval. Since fifty percent of the signal period is utilized to deliver the signal used as a reference, the DCSK technology has poor spectrum and energy consumption, lowered data information rate, and lessened bit error rate achievement [XXI]. Over the last several years, several proposals have been put up to advance the DCSK scheme's rate of data and energy usage, like a quadratic QCSK, which symbolizes chaos shift keying [XVI], HE-DCSK, which symbolizes high-efficiency DCSK [XXXVII], which symbolizes Reference-DCSK [XXXVIII], short reference based on DCSK (SR-DCSK) [XXIV], and its enhanced variants [XXXVI], and the Noise Reduction DCSK (NR-DCSK) scheme [II]. Also, in an effort to make the DCSK technology more practical and efficient, scientists attempted to remove lines of delay and accomplish legal data flows at greater rates. Multi-Carrier constructed using DCSK (MC-DCSK), a parallel development of DCSK, was established in [I-X] to enhance bandwidth and power consumption by broadcasting the chaotic reference pattern over a redirected carrier while supplying the modulating bits of data by using other carriers. An innovative method called Orthogonal Frequency Division Multiplexing DCSK (OFDM-DCSK) resolves delay line problems and improves information bit speed [XXVII]. One effective method for creating technologies with greater data transmission capacity than current systems is index modulation (IM). With its simplified hardware requirements, energy savings, and spectrum economy, it is seen as a formidable candidate for the next generation of communications networks. IM techniques can alter the state of various transfer entities, including radio frequencies, relays, send antennas, spreading codes, subcarrier networks, types of modulation, time slots, and more, in order to map data bit values. By transferring power from inactive communication items to active ones, we can reduce errors even more than with traditional systems. Without introducing any new hardware difficulties, IM can effectively boost an architecture's spectrum performance [XI-XX] efficiency, system complexity, and data rate are further examined in Section 4. In Section 5, we see the outcomes of the simulation and analyze them. Section 6 concludes with a brief overview of the study.

II. Related Works

Two versions of the CI-DCSK, which symbolizes Carrier index DCSK, technology were suggested in [X]; they combine IM with multi-carrier. One subcarrier carries the CI-DCSK1 reference chaotic signal. When DCSK modulates

the message bit and sends it over one working subcarrier while the others are dormant, the system's spectrum efficiency drops. As an upgrade over its predecessor, CI-DCSK2 uses mapped bits to designate one subcarrier as dormant. The remainder of the subcarriers transport modulated words and reference patterns. A two-layer CI-DCSK (2CI-DCSK) technology was introduced in [XIII] to advance the power consumption and spectrum of CI-DCSK1. A single subcarrier carries the reference sequence, and the bits of information are separated into two distinct sets according to: one set is combined with the reference sequence, while their Hilbert copy transfers the other set. An active subcarrier receives the modulated bit from each group's mapped bits. In the (CCI-DCSK) framework, IM maps further bits in different commutated forms of the reference chaotic waveform [XIX]. With this method, data can be transmitted in just one time period with improved spectrum and power consumption thanks to the orthogonality between reference and data patterns. To enhance privacy of data, energy conservation, and bandwidth effectiveness, the PI-DCSK, which symbolizes Permutation Index DCSK, technology was suggested by [XX]. In the second time window, the localized bits are employed to obtain a permuted duplicate of the chaotic sequence, which spreads the modulated bit across specified reference permutations. Expanding PI-DCSK was done in [I, XXI-XXX] to make it more effective. A GCI-DCSK, which symbolizes Generalized CI-DCSK, approach was introduced in [X] that periodically alters both index bits and carriers to improve CI-DCSK. When using this method, carrier indices are not restricted to orders of 2. Improved performance in power, bandwidth, and system mistakes is a result of this. The basic DCSK approach was paired with dual-index modulation to create DCSK-DIM2 and DCSK-DIM1, as suggested in [VIII]. In DCSK-DIM2 and DCSK-DIM1, the localized bits in every layer are utilized as indices for the currently used or idle periods, respectively, rather than the subcarrier. This method is comparable to 2CI-DCSK. A disadvantage is that the system can only support a single carrier, rather than supporting multiple subcarriers. Presented the M-ary DCSK system that combines carrier-code index modulation and proposed it in [VI]. Because it is not coherent, this system can skip the steps of CFIM that involve equalizing and estimating data on channel state [II]. There is a drawback to this intricate process. An M-ary DCSK with IM (IM-MDCSK) gadget that reduces power consumption and increases data speed is introduced in [VII]. At both the initial and second periods of the information structure, the system provides chaotic reference pulses and data-bearing patterns. Finally, mixed-value mapping chooses an effective indication after M-ary DCSK indicates control sequences. The receiver may be able to pinpoint busy times by looking at the absolute values of the decision components. A high-data-rate modulation system called the HDR CI-DCSK is presented in [XXXIX]. It broadcasts numerous data phases with a reference chaotic phase. Walsh sequences modulate indices and convey them using different subcarriers. Energy, bandwidth, and information rate can be enhanced by adding or removing data waves. Noise is reduced through signal repetition. For MC-DCSK grouping according to IM, [XVII] suggested GSIM-DCSKI and GSIM-DCSKII. To handle chaotic sequences, each approach employs a single subcarrier. Each GSIM-DCSKI subgroup had a live carrier and modulated bit sent by CI-DCSK1 investigators, whereas GSIM-DCSKII made use of CI-DCSK2. When it comes to speed of data and energy savings, these schemes are better than CI-DCSK. The authors of [XXXV] suggested a hybrid IM-

MC-DCSK connection mechanism called HIM-MC-DCSK. The technology aims to efficiently transmit data while reducing energy use and optimizing spectrum usage. This setup uses signals that are orthogonal to each subcarrier to indicate whether it is active or not. To achieve rapid data transfers, frequency-time IM, which combines DCSK (CTIM-DCSK), utilizes both time and carrier equipment to convey additional bits, as proposed in [XV]. Presented DCSK communication with several dimensions of IM [XXX]. The maximization of efficiency in DCSK data transmission, power use, and spectrum utilization is the primary goal of this approach. As an indicator to send additional bits in addition to physical transmission bits, this strategy makes use of time slots, Walsh patterns, and carriers. To improve the system's power performance, spectrum usage, and data communication speed, an approach called grouping frequency-time IM-DCSK (GFTIM-DCSK-I) is suggested in [XLI], which uses the material of the carrier as an indicator factor. This method is an upgrade from the one described in [XV]. The NN-IM-DCSK discovery technique in [XIV] uses neural networks to enhance indexed bits in IM-DCSK and decrease BER. Pulse position modulation IM-DCSK, CI, and Code IM designs are all compatible with this approach. The system employs a bilayer long-term short-term memory portion and many completely connected layers to improve communication dependability while gathering IM-DCSK properties and interconnections.

In this study, we extend the Generalized CI-DCSK (GCI-DCSK) technique from [X] by creating and using permuted copies of the reference chaotic series with quasi-orthogonal characteristics to disperse the modulated bit in each operational carrier. Among the results is an improvement in the system's performance regarding energy and spectrum functionality, as well as a boost in the data rate. Because each variant of the chaotic sequence is selected using the permuted index bits. Additionally, instead of correlation detection, the receiving side of the suggested work uses greedy detection to simplify the given system. Here, in brief, are the main contributions that this research has introduced.

This study proposes a new system named Generalized Joint Permutation- Carrier Index Modulation Based MC-DCSK (GJPC-IM-MCDCSK) to progress the energy savings, spectral effectiveness, and data rate of the GCI-DCSK technology that was previously described in [X]. Once the N_c busy carriers have been chosen using a combination function along with p_c carrier index bits, permutation techniques are used to generate 2^{p_p} quasi-orthogonal forms of the reference chaotic pattern. From these versions, a single sequence is chosen for each busy carrier using p_p permutation index bits to distribute its modulated bit beforehand it passes via the channel. The GJPC-IM-MCDCSK method increases the total amount of transmitted bits for the GCI-DCSK scheme to $p_c + N_c p_p + N_c$.

For the purpose of reducing the level of complexity associated with the new system, it has been suggested that the greedy detection approach be used on its receiving side rather than the correlation detection technique.

To more clearly show the superior performance of our design, we perform an analysis of the spectral efficiency, complexity, and data rate of the suggested GJPC-IM-

MCDCSK system in comparison to the MC-DCSK, CI-DCSK1, and GCI-DCSK technologies.

To substantiate our design's superiority, we compute the simulated BER effectiveness for the suggested GJPC-IM-MCDCSK scheme and compare it to traditional technologies such as GCI-DCSK, CI-DCSK1, and MC-DCSK systems for AWGN and multipath Rayleigh fading channels.

III. The GJPC-IM-MCDCSK Scheme's System Model

Figure 1 presents the block architecture of GJPC-IM-MCDCSK. In this framework, the overall amount of accessible subcarriers is N+1, wherein N_c subcarriers from N carriers will be engaged based on p_c carrier index bits, computed using the floor value of the binomial operation, $p_c = \lfloor log_2 C_N^{N_c} \rfloor$, where [N] signifies the floor function and $C_N^{N_c}$ represents the binomial coefficient. Subsequently, the p_c bits are transformed into symbols via a binary-to-symbol (B2S) converter, which is then processed by a combinatorial methods block that converts these symbols into a vector of active carriers comprising N_c components, denoted as $F = [F_1, F_2, F_m, \dots, F_{N_c}]$, where $F_m \in \{1, 2, \dots, N_c, m = 1, 2, \dots, N_c\}$, and $F_{m1} \neq F_{m2}$ if $m1 \neq m2$ [X-XX]. The suggested approach uses a reference chaotic wave of length β that is normalized to have zero mean and one variance to distribute the modulated bit across every operational carrier. Afterward, the reference sequence was placed into a permutation producer block, which has many preset permutation operators, to generate a variety of permuted copies of the original sequence. Every busy carrier uses its permutation index bits p_p for choosing the permutation operator that creates a permuted reference chaotic pattern. This permuted reference pattern is then utilized for spreading the modulated bit, which has been converted to b =[1,-1] rather than the original reference pattern. Then, it is carried through the live subcarrier through DCSK modification. To choose one of the preset permutation operators = $[P1, P2, ..., Pp, P2^{p_p}]$, $p = 1, 2, ..., 2^{p_p}$, the permutation bits p_p are mapped to a permutation symbol p_s , which belongs to the set [1, 2^{p_p}]. In [XXVI], the authors provide a permutation approach that generates a suitable set of permuted chaotic sequences from the reference chaotic sequence, all of which have the quasiorthogonal quality to each other. The carrier indices pickers will provide a series of $d = [d_1, d_2, ..., d_i, ...d_N]$ for each of the N accessible subcarriers, using the modulated bits as their basis. Every modulated bit for each alive carrier is separated by the choice of permuted reference series and fed into the subcarrier d_i if it is active; if otherwise, d_i will be zero. For every symbol period in this suggested framework, the total amount of bits for transferring information is $p_t = p_c + N_c p_p + N_c$. This paper utilizes the logistic map $(x_{k+1} = 1 - 2x_k^2)$, to produce the reference sequence $x_r(t)$, which is going to be delivered via the reference subcarrier at a central frequency of f_0 .

$$x_r(t) = \sum_{j=1}^{\beta} x_{r,j} \mathfrak{h}(t - kTc) \tag{1}$$

Where Tc stands for the time for each chip, and $\mathfrak{h}(t)$ represents the pulse shaping filter's impulse response with a normalization energy. The GJPC-IM-MCDCSK scheme's communication signal may be represented as

$$x_t(t) = \sum_{i=1}^{N} d_i \cos(2\pi f_i t + \theta_i) + x_r(t) \cos(2\pi f_0 t + \theta_0)$$
 (2)

where θ_i is the carrier modulation's phase angle and f_i is the i^{th} subcarrier's frequency.

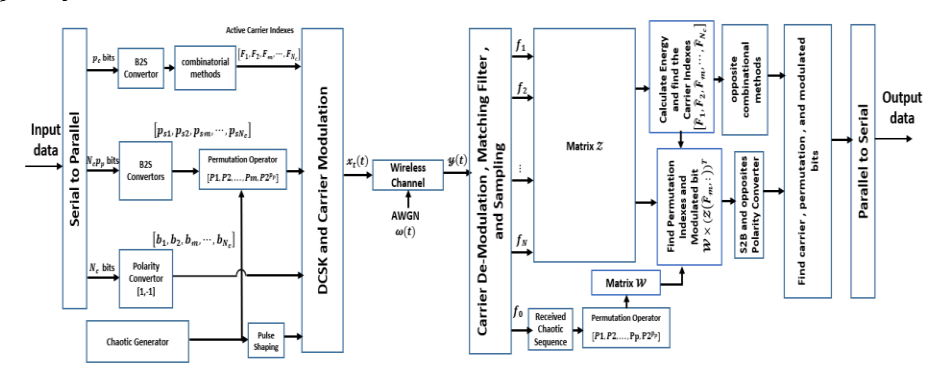


Fig. 1. The block layout for the GJPC-IM-MCDCSK scheme.

The expression for the signal that is received from the above system when subjected to the AWGN channel and L fading pathways is:

$$y(t) = \sum_{l=1}^{L} \lambda_l \delta(t - \tau_l) \otimes x_t(t) + \omega(t)$$
(3)

where λ_l represents the l^{th} channel component and l represents the latency of the route, while L represents the quantity of fading pathways. The broadband AWGN wave with a zero mean value and power spectral density of No/2 is denoted by $\omega(t)$, while the convolution assignment is represented by the symbol \otimes . It is expected that the channel coefficients λ_l will follow a separate Rayleigh pattern and be a random variable.

The signal received is processed sequentially at the receiver, including carrier recovery, matching filtering, and sampling processing. To create 2^{p_p} permuted copies for the obtained reference series, the discrete samples on the f_0 carriers are inserted into a permutation block for each framework. These permuted signals are then stored in a matrix \mathcal{W} of size $2^{p_p} \times \beta$, while the discrete sample sequences on the other N carriers are kept in a matrix \mathcal{Z} of size $N \times \beta$. The indices for the effective carriers in this structure are found using the greedy detection approach. The energy values, $E_{1\times N}$, for the data-bearing sequences contained in matrix \mathcal{Z} are calculated using this approach as follows:

$$E = Sum((Z \times Z)^{T}) = [E_{1}, E_{2}, ..., E_{i}, E_{N}]i = 1, ..., N,$$
(4)

Afterward, the greatest energy indices of N_c out of these values are defined; these indices represent the active carriers' locations. Then, they are sorted in ascendingly order to find the busy carrier index vector, \hat{F}_c , which may be expressed as:

$$\widehat{F}_{c} = sort(Max(E, N_{c})) = [\widehat{F}_{1}, \widehat{F}_{2}, \widehat{F}_{m}, \cdots, \widehat{F}_{N_{c}}] \widehat{F}_{m} \in 1, 2, \dots, N$$
 (5)

Lastly, the actual carrier index bits are determined by converting the previously acquired symbol \widehat{F}_c into binary with p_c bits using the inverse combinational approach. Knowing which data-bearing sequence is delivered across each passive carrier in matrix \mathcal{Z} is the first step in calculating the permutation index for this network. Using the active carrier vector that was discovered, \widehat{F}_c allows this to be achieved. Mathematical multiplication of the sequence of each active subcarrier by the matrix \mathcal{W} , which contains the 2^{p_p} permuted copies of the received reference sequence, yields the correlation matrix $\mathcal{D}_{1\times 2^{p_p}}^m$, $m\in 1,2,...,N_c$, as:

$$\mathcal{D}_{1\times 2^{\mathrm{pp}}}^{m} = \mathcal{W} \times (\mathcal{Z}(\widehat{F}_{m},:))^{T} = [\mathcal{D}_{1}^{m}, \mathcal{D}_{2}^{m}, \dots, \mathcal{D}_{2^{\mathrm{pp}}}^{m}] \widehat{F}_{m} \in \widehat{F}_{c}, m = 1, 2, \dots, N_{c}$$
 (6)

To obtain its permutation index, the following procedure is to follow: for the m^{th} active subcarrier, the greatest absolute value of the correlation matrix $\mathcal{D}^m_{1\times 2^{\operatorname{pp}}}$ is computed as:

$$\widehat{p_{s,m}} = \operatorname{Max}(|\mathcal{D}_{1\times 2}^{m}|), m = 1, \dots, N_c$$
(7)

where $\widehat{p_{s,m}}$ represents the symbol for the m^{th} active carrier's permutation index, which was transformed to binary using p_p bits. Finally, for every active subcarrier, the modulated bit is retrieved as:

$$modulated \ bit = \begin{cases} 0 & if \ sign\left(\mathcal{D}^m_{1\times 2^{\operatorname{Pp}},(\widehat{p_{\widehat{s},m}})}\right) = -1\\ 1 & if \ sign\left(\mathcal{D}^m_{1\times 2^{\operatorname{Pp}},(\widehat{p_{\widehat{s},m}})}\right) = +1 \end{cases}, m = 1, \dots, N_c \tag{8}$$

IV. System Analysis

It is possible to determine the data rate of any system by dividing the total number of bits that are communicated for each symbol by the total time interval that it takes to transmit that symbol. As a result, and in accordance with this definition, the data rate for the system that is being proposed is equal to $\frac{p_c + N_c p_p + N_c}{\beta T c}$, where $\beta T c$ is the time period for sending one symbol. Comparatively speaking, the data rate for traditional systems such as GCI-DCSK [X], CI-DCSK1 [XII], and MC-DCSK [XXII] is equivalent to $\frac{p_c + N_c}{\beta T c}$, $\frac{\log_2(N) + 1}{\beta T c}$, and $\frac{N}{\beta T c}$, respectively.

Figure 2 illustrates the influence of the number of active carriers on the data rate of the suggested system, utilizing two distinct values of permutation index bits for each active carrier, in comparison to competing systems, the following parameters are set: N=16, N_c ranging from 2 to 14, $p_p=2,3$, and $\beta=128$. This figure indicates that the proposed system attains a higher data rate than existing systems, attributable to the employment of additional permutation index bits alongside working carrier index bits, which facilitates the transmission of more data within the symbol period than competing systems. This figure also indicates that, for a constant number of active carriers, the data rate for the proposed system increases as the number of permutation index bits per active carrier rises. In addition, the data rates of CI-DCSK1 and MC-DCSK systems are the same for all values of N_c , as they are independent of it.

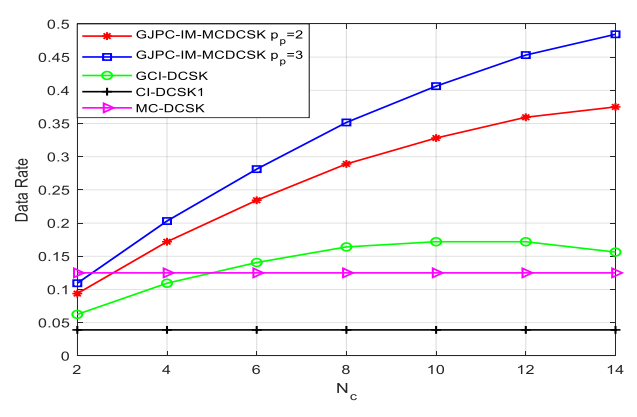


Fig. 2. Data rate for the suggested system in comparison with other conventional DCSK systems at different values of N_c and p_p .

Spectrum efficiency is a critical metric that quantifies the effectiveness of a system in utilizing the designated spectrum relative to conventional solutions. The calculation is derived from the ratio of bits transmitted per unit time within the designated spectrum of the system. Considering that each subcarrier's bandwidth is consistent and denoted by B, the spectral efficiency of the GJPC-IM-MCDCSK system is calculated as $\frac{p_c+N_cp_p+N_c}{\beta Tc(N+1)B}$. In contrast, the spectral efficiencies for GCI-DCSK [X], CI-DCSK1 [X-XX], and MC-DCSK [16] are $\frac{p_c+N_c}{\beta Tc(N+1)B}$, $\frac{\log_2(N)+1}{\beta Tc(N+1)B}$, and $\frac{N}{\beta Tc(N+1)B}$, respectively.

Figure 3 shows the comparison of spectral efficiency between the suggested system and traditional systems, utilizing the identical parameters as those in Figure 2. The suggested strategy appears to utilize the spectrum more efficiently than the alternative schemes, as it transmits a greater number of data bits with each symbol. Furthermore, as previously indicated, this performance improves with increasing N_c and p_p . This is because when the number of active carriers and permutation bits increases, the amount of data bits transmitted in each symbol also escalates.

The examination of computational complexity relies on the aggregate quantity of multiplications executed for spreading and despreading a single bit throughout one symbol period. In GJPC-IM-MCDCSK, the transmitter executes, N_c β spreading operations to transmit a symbol that encompasses $p_c + N_c p_p + N_c$ bits. Due to the implementation of greedy detection at the receiver, $(N\beta + N_c 2^{p_p}\beta)$ correlations are conducted to retrieve the symbol. Additionally, $N\beta$ multiplications are necessary to ascertain the indices of the N_c active carriers are utilized to recover the carrier index bits. Conversely, $N_c 2^{p_p}\beta$ correlation is used to calculate the modulated bits and permutation index bits for each active carrier. Hence, the sum of all the multiplications needed for the GJPC-IM-MCDCSK system for one bit during one symbol duration is $\frac{N_c \beta + N\beta + N_c 2^{p_p}\beta}{p_c + N_c p_p + N_c}$, whereas for GCI-DCSK [X], CI-DCSK1 [XII], and MC-DCSK [16], it is $\left(\frac{N_c \beta + N\beta}{p_c + N_c}, \frac{\beta + N}{\log_2(N) + 1}\right)$, and $\frac{2N\beta}{N}$, respectively. The amount of multiplications per bit required for the suggested system, when utilizing correlation

detection, is expressed as $\left(\frac{N_c \beta + N_2^{p_p} \beta}{p_c + N_c p_p + N_c}\right)$, resulting in increased complexity compared to greedy detection.

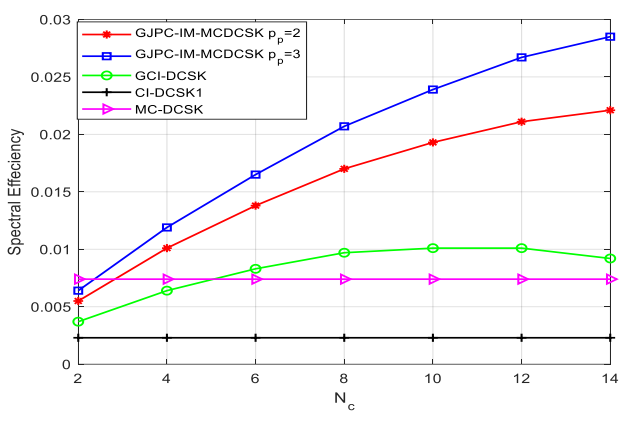


Fig. 3. Spectrum efficiency for the proposed system in comparison with other conventional DCSK systems at different values of N_c and p_v .

Figures 4 and 5 contrast the proposed system's complexity against alternative DCSK architectures regarding the total number of multiplication operators and the total number of multiplications per bit, respectively, utilizing the same parameters as Figure 2. Figure 4 demonstrates that the proposed system employing greedy detection exhibits heightened complexity compared to alternative systems, due to the utilization of $N_c 2^{p_p} \beta$ multiplications on the receiving end to recover the permutation index bits for each active carrier, with this complexity intensifying as the number of permutation index bits per active carrier increases. This figure also indicates that the proposed system, utilizing a correlation detector, is more complex than employing greedy detection. This is because each carrier at the receiver side requires $N2^{p_p}\beta$ multiplications to ascertain the indices of active carriers and their permutation indices, whereas greedy detection necessitates only $N\beta + N_c 2^{p_p}\beta$ operations to recover the active carrier and permutation index bits. Conversely, as the multiplication required for each bit increases, Figure 5 illustrates that the proposed system exhibits greater complexity per bit than the GCI-DCSK scheme. This complexity escalates with the increase in the number of permutation index bits for each active carrier, despite the fact that the proposed system transmits more bits than the GCI-DCSK system. Furthermore, this figure indicates that the proposed system exhibits lower complexity per bit than MC-DCSK at two specific values of permutation index bits. This is attributed to the greater number of operations required at the transmitter for MC-DCSK, coupled with its reduced number of transmitted bits per symbol duration compared to the proposed system, resulting in a higher multiplication per bit for MC-DCSK. Moreover, the suggested system exhibits reduced complexity compared to CI-DCSK1 at $p_p = 2$, as the quantity of transmitted bits per symbol duration exceeds that of CI-DCSK1. The complexity per bit of the suggested system utilizing a correlation detector is greater than that of greedy detection, and it diminishes as the quantity of transmitted bits per symbol increases with the rise in active carriers.

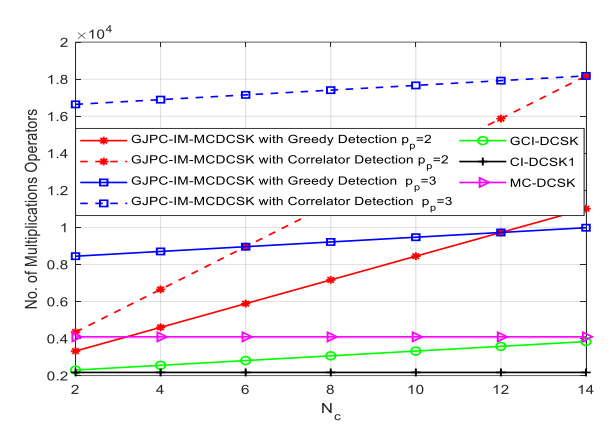


Figure 4. Number of multiplication operators for the proposed system in relation to other conventional DCSK systems at different values of N_c and p_p .

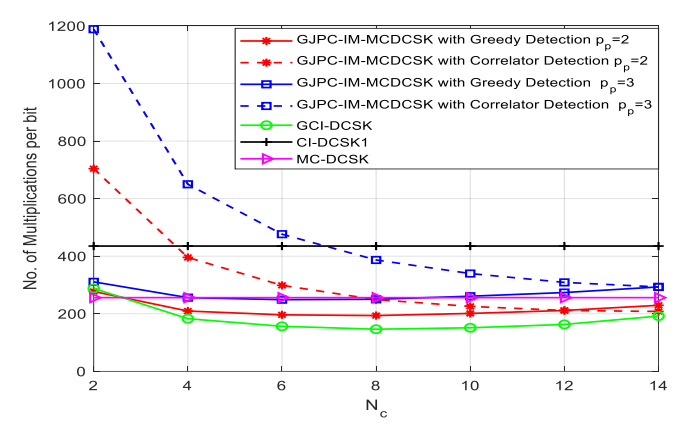


Fig. 5. Number of multiplication operators per bit for the proposed system in relation to other conventional DCSK systems at various values of N_c and p_p .

V. Simulation Results

This section presents the BER, symbolizing Bit Error Rate, performance of the suggested GJPC-IM-MCDCSK system under the influence of AWGN channel and Rayleigh fading channels with three routes. The system is characterized by an average power gain of 1/3 and chip time delays equal to 0, 2, and 5 for the first, second, and third paths, respectively. It also shows how this approach compares to GCI-DCSK, CI-DCSK1, and MC-DCSK regarding BER performance. The MATLAB software, namely version 2018a, is used to compute the numerical findings.

With about the same amount of data bits conveyed over a single symbol period while dealing with the effects of AWGN and multipath channels, the BER performance of GCI-DCSK and the proposed system is contrasted in Figure 6. In contrast to the GCI-DCSK system, which uses 17 bits, N=16, and N_c =5, the suggested systems use 16 bits per symbol period, N_c =2, and p_p =4. The figure clearly shows that GJPC-IM-MCDCSK outperforms GCI-DCSK in terms of performance. At BER equal to

10⁻², for AWGN channels, the gain is approximately 2 dB, and for fading channels, it's about 1 dB. The reason is, achieving a certain performance for BER requires less energy when using permutation index bits for each activated carrier, which boosts the quantity of bits mapped on a single symbol and reduces the value of Eb/No. Fewer active carriers are required for broadcast data bits compared to GCI-DCSK, which results in fewer modulated bits transmitted for each symbol interval and less noise corruption.

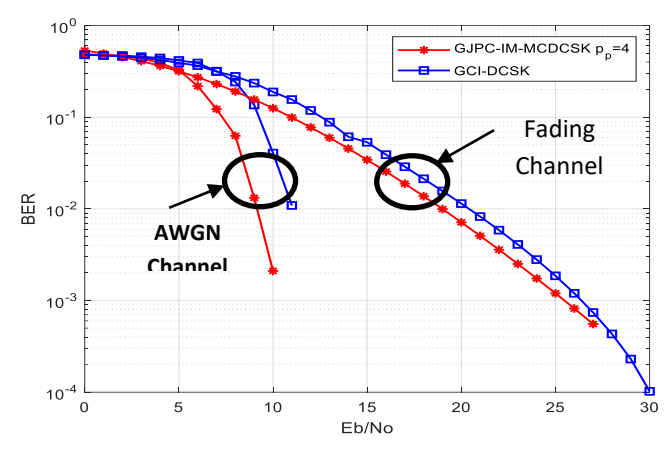


Fig. 6. BER Comparisons between GJPC-IM-MCDCSK and GCI-DCSK systems under AWGN and multipath channels and $\beta = 128$.

System	No. of delivered data bits
GJPC-IM-MCDCSK	37 bits, at $N_c = 8$, $p_p = 2$, $p_c = 13$
	45 bits, at $N_c = 8$, $p_p = 3$, $p_c = 13$
GCI-DCSK	21 bits, at $N_c = 8$, $p_c = 13$
CI-DCSK1	5 bits, at $p_c = 4$
MC-DCSK	16 bits

Table 1. Number of transmitted bits in each symbol duration.

Figure 7 compares the BER results of the system that is suggested with those of the GCI-DCSK, CI-DCSK1, and MC-DCSK structures in the presence of AWGN and Rayleigh fading channels. With β =128 and N=16 subcarriers, the comparison is carried out. For each symbol duration, Table 1 lists the aggregate number of data bits delivered by each system.

At the BER level 10^{-2} in the AWGN and multipath channels, this figure reveals that the effective BER of GJPC-IM-MCDCSK drops around 1 dB as p_p increases. Not only that, but the figure clearly shows that the GJPC-IM-MCDCSK outperforms the competition. The reason is that, as demonstrated in Table 1, using permutation index bits for every active carrier reduces the BER value and causes a reduction in the energy consumption for the modulated bit. Additionally, it transmits more data per symbol duration than competing systems. Consequences of these outcomes can be developed with [XL-XLVI].

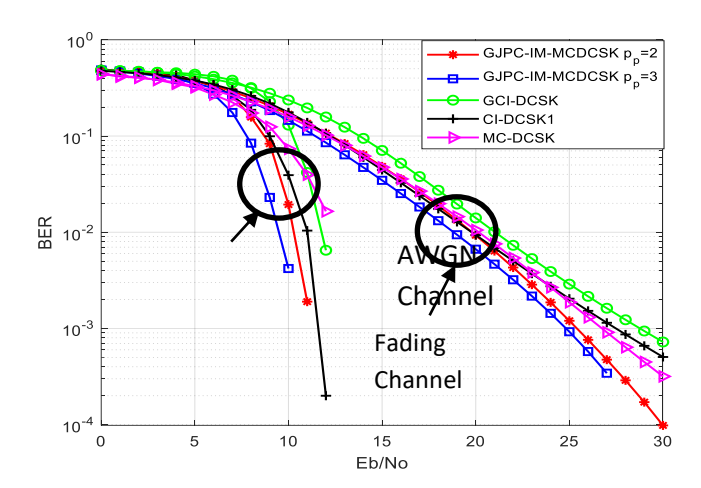


Fig. 7. BER Comparisons between GJPC-IM-MCDCSK and other DCSK schemes.

VI. Conclusions

This research presents a novel system that is referred to as GJPC-IM-MCDCSK. The purpose of this system is to advance the efficiency of the GCI-DCSK technology in terms of energy savings, spectrum effectiveness, and data rate. The system employs permutation techniques to construct quasi-orthogonal versions of the reference chaotic pattern. A single sequence is selected for each busy carrier by making use of p_p permutation index bits. The GJPC-IM-MCDCSK technique can enhance the total number of bits transferred for the GCI-DCSK scheme. The greedy detection strategy should be used to decrease complexity. The proposed system's examination regarding BER, spectral efficiency, and data rate demonstrates that it attains a greater data rate and spectral efficiency relative to current systems, in addition to outperforming the competition in terms of BER performance. This results from the utilization of supplementary permutation index bits in conjunction with operational carrier index bits. For future work, the time domain combined with the frequency domain is suggested to be used to convey more data bits than the proposed system.

Conflict of Interest

The authors declare that there is no conflict of interest regarding this paper.

References

- I. Al Bassam, N., & Al-Jerew, O. (2021). Design and implementation of enhanced permutation index differential chaos shift keying system. Physical Communication, 46, 101312. 10.1016/j.phycom.2021.101312
- II. Au, M., Kaddoum, G., Alam, M. S., Başar, E., & Gagnon, F. (2019). Joint code-frequency index modulation for IoT and multi-user communications. IEEE Journal of Selected Topics in Signal Processing, 13, 1223–1236. 10.1109/JSTSP.2019.2933056

- III. Bai, C., Ren, H. P., & Grebogi, C. (2019). Experimental phase separation differential chaos shift keying wireless communication based on matched filter. IEEE Access, 7, 25274–25287. 10.1109/ACCESS.2019.2900729
- IV. Basar, E., Wen, M., Mesleh, R., Di Renzo, M., Xiao, Y., & Haas, H. (2017). Index modulation techniques for next-generation wireless networks. IEEE Access, 5, 16693–16746. 10.1109/ACCESS.2017.2737528
- V. Başar, E., Aygölü, Ü., Panayırcı, E., & Poor, H. V. (2013). Orthogonal frequency division multiplexing with index modulation. IEEE Transactions on Signal Processing, 61, 5536–5549. 10.1109/TSP.2013.2279771
- VI. Cai, X., Xu, W., Lau, F. C. M., & Wang, L. (2020). Joint carrier-code index modulation aided M-ary differential chaos shift keying system. IEEE Transactions on Vehicular Technology, 69, 15486–15499. 10.1109/TVT.2020.3041927
- VII. Cai, X., Xu, W., Miao, M., & Wang, L. (2020). Design and performance analysis of a new M-ary differential chaos shift keying with index modulation. IEEE Transactions on Wireless Communications, 19, 846–858. 10.1109/TWC.2019.2949315
- VIII. Cai, X., Xu, W., Wang, L., & Xu, F. (2019). Design and performance analysis of differential chaos shift keying system with dual-index modulation. IEEE Access, 7, 26867–26880. 10.1109/ACCESS.2019.2901016
 - IX. Chen, H., Chen, P., Wang, S., Lai, S., & Chen, R. (2022). Reference-modulated PI-DCSK: A new efficient chaotic permutation index modulation scheme. IEEE Transactions on Vehicular Technology, 71, 9663–9673. 10.1109/TVT.2022.3181180
 - X. Cheng, G., Chen, X., Liu, W., & Xiao, W. (2019). GCI-DCSK: Generalized carrier index differential chaos shift keying modulation. IEEE Communications Letters, 23, 2012–2016. 10.1109/LCOMM.2019.2933827
 - XI. Cheng, G., Wang, L., Chen, Q., & Chen, G. (2018). Design and performance analysis of generalised carrier index M-ary differential chaos shift keying modulation. IET Communications, 12, 1324–1331. 10.1049/iet-com.2017.0800
- XII. Cheng, G., Wang, L., Xu, W., & Chen, G. (2017). Carrier index differential chaos shift keying modulation. IEEE Transactions on Circuits and Systems II: Express Briefs, 64, 907–911. 10.1109/TCSII.2016.2613093
- XIII. Dai, W., Yang, H., Song, Y., & Jiang, G. (2018). Two-layer carrier index modulation scheme based on differential chaos shift keying. IEEE Access, 6, 56433–56444. 10.1109/ACCESS.2018.2872748
- XIV. Fang, Y., Peng, D., Ma, H., Han, G., & Li, Y. (2024). A neural network-aided detection scheme for index-modulation DCSK system. IEEE Transactions on Vehicular Technology, 73, 2109–2121. 10.1109/TVT.2023.3313813

- XV. Fang, Y., Zhuo, J., Ma, H., Mumtaz, S., & Li, Y. (2023). Design and analysis of a new index-modulation-aided DCSK system with frequency-and-time resources. IEEE Transactions on Vehicular Technology, 72, 7411–7425. 10.1109/TVT.2023.3238379
- XVI. Galias, Z., & Maggio, G. M. (2001). Quadrature chaos-shift keying: Theory and performance analysis. IEEE Transactions on Circuits and Systems I: Fundamental Theory and Applications, 48, 1510–1519. 10.1109/TCSI.2001.972858
- XVII. Hasan, F. S. (2021). Design and analysis of grouping subcarrier index modulation for differential chaos shift keying communication system. Physical Communication, 47, 101325. 10.1016/j.phycom.2021.101325
- XVIII. Hasan, F. S., & Fahad, H. F. (2020). Design and analysis of an OFDM-based orthogonal multilevel code-shifted differential chaos shift keying. Indonesian Journal of Electrical Engineering and Computer Science, 20, 1369–1378. 10.11591/ijeecs.v20.i3.pp1369-1378
 - XIX. Herceg, M., Vranjes, D., Kaddoum, G., & Soujeri, E. (2018). Commutation code index DCSK modulation technique for high-data-rate communication systems. IEEE Transactions on Circuits and Systems II: Express Briefs, 65, 1954–1958. 10.1109/TCSII.2018.2817930
 - XX. Herceg, M., Kaddoum, G., Vranjes, D., & Soujeri, E. (2018). Permutation index DCSK modulation technique for secure multiuser high-data-rate communication systems. IEEE Transactions on Vehicular Technology, 67, 2997–3011. 10.1109/TVT.2017.2774108
 - XXI. Huang, T., Wang, L., Xu, W., & Lau, F. C. M. (2016). Multilevel code-shifted differential-chaos-shift-keying system. IET Communications, 10, 1189–1195. 10.1049/iet-com.2015.1109
- XXII. Kaddoum, G., Richardson, F.-D., & Gagnon, F. (2013). Design and analysis of a multi-carrier differential chaos shift keying communication system. IEEE Transactions on Communications, 61, 3281–3291. 10.1109/TCOMM.2013.071013.130225
- XXIII. Kaddoum, G., Soujeri, E. (2016). NR-DCSK: A noise reduction differential chaos shift keying system. IEEE Transactions on Circuits and Systems II: Express Briefs, 63, 648–652. 10.1109/TCSII.2016.2532041
- XXIV. Kaddoum, G., Soujeri, E., & Nijsure, Y. (2016). Design of a short reference noncoherent chaos-based communication systems. IEEE Transactions on Communications, 64, 680–689. 10.1109/TCOMM.2015.2514089
- XXV. Kaddoum, G., Tran, H.-V., Kong, L., & Atallah, M. (2017). Design of simultaneous wireless information and power transfer scheme for short reference DCSK communication systems. IEEE Transactions on Communications, 65, 431–443. 10.1109/TCOMM.2016.2619707

- XXVI. Lau, F. C. M., Cheong, K. Y., & Tse, C. K. (2003). Permutation-based DCSK and multiple-access DCSK systems. IEEE Transactions on Circuits and Systems I: Fundamental Theory and Applications, 50, 733–742. 10.1109/TCSI.2003.812616
- XXVII. Li, S., Zhao, Y., & Wu, Z. (2015). Design and analysis of an OFDM-based differential chaos shift keying communication system. Journal of Communications, 10, 199–205. 10.12720/jcm.10.3.199-205
- XXVIII. Liu, S., Chen, P., & Chen, G. (2021). Differential permutation index DCSK modulation for chaotic communication system. IEEE Communications Letters, 25, 2029–2033
 - XXIX. Luo, R., Yang, H., Meng, C., & Zhang, X. (2022). A novel SR-DCSK-based ambient backscatter communication system. IEEE Transactions on Circuits and Systems II: Express Briefs, 69, 1707–1711. 10.1109/TCSII.2021.3109020
 - XXX. Ma, H., Fang, Y., Chen, P., Mumtaz, S., & Li, Y. (2023). A novel differential chaos shift keying scheme with multidimensional index modulation. IEEE Transactions on Wireless Communications. 10.1109/TWC.2022.3192347
 - XXXI. Nazar, B., & Hasan, F. S. (2023). Joint grouping subcarrier and permutation index modulations based differential chaos shift keying system. Physical Communication, 61, 102213. 10.1016/j.phycom.2023.102213
- XXXII. Nazar, B., & Hasan, F. S. (2024). Enhanced two-way cooperative DCSK system via grouping subcarrier-permutation index modulation. In Evolution in Signal Processing and Telecommunication Networks (pp. 23–35). Springer. 10.1007/978-981-97-0644-0 3
- XXXIII. Nazar, B., & Hasan, F. S. (2024). Performance analysis of two-way multi-users cooperative communication system based on GSPIM-DCSK scheme. AEU, International Journal of Electronics and Communications, 178, 155303. 10.1016/j.aeue.2024.155303
- XXXIV. Sui, T., Feng, Y., Jiang, Q., Liu, F., & Zhang, T. (2022). Design and analysis of a short reference orthogonal double bit rate differential chaotic shift keying communication scheme. Electronics, 11. 10.3390/electronics11132020
- XXXV. Tao, Y., Fang, Y., Ma, H., Mumtaz, S., & Guizani, M. (2022). Multi-carrier DCSK with hybrid index modulation: A new perspective on frequency-index-aided chaotic communication. IEEE Transactions on Communications, 70, 3760–3773. 10.1109/TCOMM.2022.3169214
- XXXVI. Xu, W., & Wang, L. (2017, October 20–23). Performance optimization for short reference differential chaos shift keying scheme. In Proceedings of the IEEE International Conference on Signal Processing, Communications and Computing (ICSPCC) (pp. 1–6). 10.1109/ICSPCC.2017.8242434
- XXXVII. G. P. High-efficiency Yang, Н., & Jiang, (2012).differential-chaos-shift-keying scheme for chaos-based noncoherent communication. IEEE Transactions on Circuits and Systems II: Express Briefs, 59, 312–316. 10.1109/TCSII.2012.2190859

- XXXVIII. Yang, H., & Jiang, G. P. (2013). Reference-modulated DCSK: A novel chaotic communication scheme. IEEE Transactions on Circuits and Systems II: Express Briefs, 60, 232–236. 10.1109/TCSII.2013.2251949
 - XXXIX. Yang, H., Xu, S. Y., & Jiang, G. P. (2021). A high data rate solution for differential chaos shift keying based on carrier index modulation. IEEE Transactions on Circuits and Systems II: Express Briefs, 68, 1487–1491. 10.1109/TCSII.2020.3038163
 - XL. Yao, W., Zhang, X., Wang, J., Li, Z., Li, J., & Song, H. (2023, May). Design and analysis of a noise reduction PI-DCSK system for wireless underground power pipe gallery communications. In Proceedings of the 2023 4th Information Communication Technologies Conference (ICTC) (pp. 44–48). 10.1109/ICTC57116.2023.10154786
 - XLI. Yaseen, R. A., & Hasan, F. S. (2024). Design and analysis of grouping active subcarrier frequency-time index modulation for differential chaos shift keying communication system. Journal of Communications Software and Systems, 20, 173–185. 10.24138/jcomss-2023-0182
 - XLII. Yaqeen S.Mezaal, Halil T. Eyyuboğlu, and Jawad K. Ali. "New microstrip bandpass filter designs based on stepped impedance Hilbert fractal resonators." IETE Journal of Research 60.3 (2014): 257-264.
 - XLIII. Y. S. Mezaal, L. N. Yousif, Z. J. Abdulkareem, H. A. Hussein, and S. K. Khaleel, "Review about effects of IoT and nanotechnology techniques in the development of IoNT in wireless systems," *International Journal of Engineering and Technology*, vol. 7, no. 4, pp. 3602–3606, 2018. 10.14419/ijet.v7i4.19615..
 - XLIV. Yahya, A., J. A. Aldhaibaini, R. B. Ahmad, Z. G. Ali, and R. A. Fayadh, "Enhancing link quality in a multi-hop relay in LTE-A employing directional antenna," in 2013 IEEE International RF and Microwave Conference (RFM), 2013. 10.1109/RFM.2013.6757227
 - XLV. Yahya, A., J. A. Aldhaibaini, R. B. Ahmad, M. Zain, and A. S. Salman, "PERFORMANCE ANALYSIS OF TWO-WAY MULTI-USER WITH BALANCE TRANSMITTED POWER OF RELAY IN LTE-A CELLULAR NETWORKS," Journal of Theoretical & Applied Information Technology, vol. 51, no. 2, 2013.
 - XLVI. Zainab Falih Hamza, et. al. "Estimating systems reliability functions for the generalized exponential distribution with application", *Period. Eng. Nat. Sci.*, vol. 11, no. 3, pp. 108–114, May 2023, 10.21533/pen.v11.i3.138